

Numerical characterization of the Douro River plume

R. Mendes^{1,2*}, N. Vaz², M. C. Sousa², J. G. Rodrigues³, M. deCastro⁴, J. M. Dias²

¹CIIMAR, University of Porto, 4099-002 Porto, Portugal

²CESAM, Physics Department, University of Aveiro, 3810-193 Aveiro, Portugal

³HIDROMOD, Rua Teles Palhinha, 4, 2740-278 Porto Salvo, Portugal

⁴EPhysLab, Universidade de Vigo, Facultade de Ciencias, Ourense, Spain

rpsm@ua.pt

Abstract. The Douro is one of the largest rivers of the Iberian Peninsula, representing the most important buoyancy source into the Atlantic Ocean on the north-western Portuguese coast. The main goal of this study is to contribute to the knowledge of physical processes associated with the propagation of the Douro River plume. The general patterns of dispersion in the ocean and how the plume change hydrography and coastal circulation were evaluated, considering the main drivers involved: river discharge and wind. Coastal models were implemented to characterize the propagation of the plume, its dynamics, and its impact on coastal circulation. Different numerical scenarios of wind and river discharge were analyzed. The estuarine outflow is sufficient to generate a northward coastal current without wind under moderate-to-high river discharge conditions. Under easterly winds, the propagation pattern is similar to the no wind forcing, with a northward current speed increasing. A southward coastal current is generated only by strong westerly winds. Under upwelling-favorable (northerly) winds, the plume extends offshore with tilting towards the southwest. Southerly winds increase the velocity of the northward current, being the merging of the Douro and Minho estuarine plumes a likely consequence.

Keywords: Estuary; Coastal Circulation; NW Iberian Peninsula; MoHid

1 Introduction

River plumes are flow structures, which can occur in a range of sizes and shapes and that impact the coastal ocean, changing local flow and water properties concentration. They represent a significant link between terrestrial and marine systems, affecting densely populated areas. Therefore, understanding the processes that determine the transport of estuarine waters is essential to know the fate and transport of solute and particulate materials across the land-sea interface. The propagation of estuarine waters along the coast can be influenced by several external forcing, which includes Earth rotation represented by the Coriolis force, tides, winds, freshwater discharge, and ambient flows [1].

The propagation of the Douro River plume has a high impact on the coastal hydrography of NW of Portugal [2]. This plume promotes buoyant water transport in the downstream direction. Recently, the interaction between the Douro and Minho estuarine

plumes under southerly winds was studied through numerical simulations[2], revealing an indirect role of the Douro plume on both plumes' fate over the shelf.

The aim of this study is to analyze the horizontal plume propagation under different wind direction and river discharge scenarios by means of validated simulations using a MOHID (www.mohid.com) model implementation developed for this coastal area.

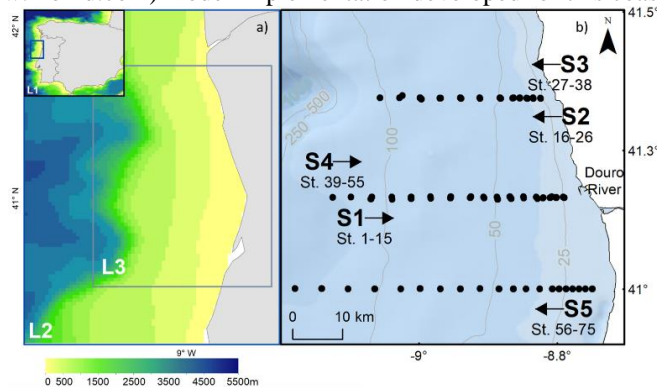


Fig. 1. - (a) Study area and the MOHID nesting domains (b) Location of the CTD sampling stations (black dots) during the 2007 survey at five zonal sections (S). Note: CTD sampling stations at S1 and S4, and S2 and S3 were performed at the same locations but at different times.

2 Data and Methods

2.1 Model Configuration

The implementation of the numerical model MOHID to the region influenced by the Douro plume follows a nested downscaling methodology similar to that previously validated for the NW coast of the Iberian Peninsula [3].

This nested model comprises a large domain to compute the barotropic tide (L1) and two smaller baroclinic domains (L2 and L3). The third level comprises a smaller region with higher horizontal resolution (Fig. 1a).

The first level (L1) ranged from 13.5°W to 1°E and 33.5°N to 50°N, with a variable horizontal resolution of 0.06° (~6 km) and was constructed based on the ETOPO1 global database. This level is a 2D model using the thoroughly revised tidal solution from a global hydrodynamic model (FES2012) as a boundary condition [4], which constitutes an update to the previous coastal application [3], which used an older dataset. The tidal reference solution generated by this model is then propagated to the subsequent 3D baroclinic levels applying the radiation scheme[5]. The time step was 180 s, and the horizontal eddy viscosity was 100 m² s⁻¹.

L2 and L3 levels are focused on the Douro Estuary and were built based on GEBCO bathymetries [6]. L2 domain ranges from 9.94°W to 8.40°W and 40.16°N to 42.10°N, with a horizontal resolution of ~2 km and L3 ranges from 9.52°W to 8.60°W and 40.50°N to 41.75°N, with a horizontal resolution of ~500 m. The initial ocean stratification in L2 and L3 was set through 3D monthly mean climatological fields of water temperature and salinity from the World of Ocean Atlas 2013 [7]. Following [3], the baroclinic forcing was slowly activated over ten inertial periods, and the biharmonic

filter coefficients were set to $1 \times 10^7 \text{ m}^4 \text{ s}^{-1}$ and $1 \times 10^4 \text{ m}^4 \text{ s}^{-1}$ for L2 and L3, respectively. A time step of 60 s was used in L2 domain with a turbulent horizontal eddy viscosity set to $20 \text{ m}^2 \text{ s}^{-1}$. The time step and turbulent horizontal eddy viscosity were set to 60 s and $5 \text{ m}^2 \text{ s}^{-1}$, respectively in the L3. A z-level vertical discretization was adopted using Cartesian coordinates. Considering the surface behavior of estuarine plumes and the importance of the baroclinic processes on their dispersion, sigma coordinates were applied on the first 10 m.

The 3D momentum, heat and salt balance equations were computed implicitly in the vertical direction and explicitly in the horizontal direction. All ocean boundary conditions at L3 domain were supplied by hydrodynamic and water properties solutions from L2 domain. A Flow Relaxation Scheme [8] was applied to water level, velocity components, water temperature and salinity in baroclinic models.

Surface boundary conditions were imposed using high-resolution results from Weather Research and Forecasting Model (WRF) with a spatial resolution of 4 km [9]. WRF output spatial fields were hourly interpolated for L2 and L3 domains, using triangulation and bilinear methods in space and time, respectively. At the surface, the sensible and latent heat fluxes were calculated using the Bowen and Dalton laws, respectively. A shear friction stress was imposed for bottom boundary condition, assuming a logarithmic velocity profile.

Douro outflows were previously computed using an estuarine model developed for the inner part of the estuary [2] and directly imposed offline as momentum, water, and mass discharge to the coastal model (L3) as a discharge point. The effects of other small rivers were not considered in this study due to their neglectable freshwater inflow [2].

2.2 Experimental Design

Built on a statistical analysis of the Douro River discharge data, three scenarios were chosen accounting the 25th, 50th and 75th percentiles of annual maxima of the month with maximum daily mean inflows - January. These percentiles correspond to low ($608 \text{ m}^3 \text{ s}^{-1}$), moderate ($1486 \text{ m}^3 \text{ s}^{-1}$) and high ($3299 \text{ m}^3 \text{ s}^{-1}$) discharge winter scenarios, respectively.

Following the method proposed by [3], the idealized scenario with high river discharge starts from the average value for January ($1055 \text{ m}^3 \text{ s}^{-1}$) and then increases exponentially under 4 days until reach $3299 \text{ m}^3 \text{ s}^{-1}$. The maximum is about three times the average. This ratio was also adopted for moderate and low discharge scenarios. The water temperature and salinity of the Douro River in the estuarine model implementation [2] were set to 8°C and 0, respectively.

The definition of wind scenarios was also based on statistical results presented by [3]. The probability of occurrence of winds with intensity lower than 3 m s^{-1} is 32 %, while the probability of moderate winds (between 3 and 6 m s^{-1}) is higher than 46 % [3]. These wind intensities were used in the simulations as representative of the prevailing wind regime in this region.

After the model validation, 27 experiments to test the plume propagation were done, including four wind directions (north, south, west, and east), two wind intensities (3 and 6 m s^{-1}) and three river discharges (high, moderate and low). Moreover, three simulations were carried out without wind. In all simulations, results were analyzed for

January 2010 after a spin-up of six months, from July 2009 to December 2009. This period was considered representative of local winter condition [2]. Wind forcing for each scenario starts when the river discharge reached its maximum.

3 Results and Discussion

3.1 Validation

A 1-month simulation was carried out for all domains from 20 January to 28 February 2007 to evaluate the coastal model accuracy. Salinity was set to 0 in the estuarine model, and temperature of freshwater inflow was set based on the daily smooth air temperature provided by WRF predictions. In situ dataset includes CTD hydrographic surveys acquired on January 24 (S1) and 26 (S2) and February 6 (S3, S4, and S5), 2007 (Black points in Fig. 1b). The adjustment between model predictions and observed data was evaluated using the Root Mean Square Error (RMSE) and Bias computation.

RMSE values for salinity range from 0.01 (St. 16) to 1.05 (St. 55) (Fig. 2). Bias range from -0.54 (St 55) to 0.22 (St. 27) being negative for the majority of stations, which indicates a model underestimation of the river plume. Significant exceptions are stations 27 and 28, where the bias are 0.22 and 0.08, respectively. In situ and modeled salinities reveal low salinity features in all sections, being Section 2 an exception, which explain a lower bias. Although the plume spreading is well simulated in front of the mouth, the model tends to overestimate the stratification, observed as a large RMSE and negative bias in Section 4.

A lower agreement is expected for water temperature because of its higher variability. The RMSE ranges from 0.16°C (St. 34) to 1.10°C (St. 42), with an average of 0.58°C considering all stations. Bias is positive for all profiles, ranging from 0.08°C (St. 37) to 0.95°C (St. 49). The model tends to underestimate observed water temperature along the water column (Figure 2). Nonetheless, the deviation range ($\sim 1^\circ\text{C}$) is low and close to that obtained by [3].

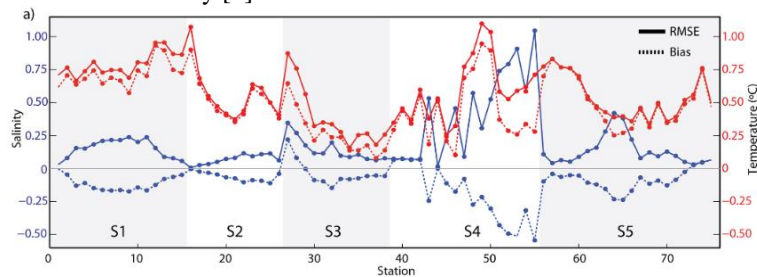


Fig. 2. RMSE and Bias between observed and predicted salinity (blue) and water temperature (red) vertical profiles from each station represented in Fig. 1b.

3.2 River Discharge Influence

The spread of the Douro plume is described in Fig. 3 under the different river discharge scenarios and without wind after nine days of simulation and five from the river inflow peak.

All figures show the advection of low salinity waters to the right due to the Coriolis effect and the extension of the river plume after establishing a geostrophic balance. Additionally, all river discharge scenarios share common features such as a re-circulating bulge in the front of the mouth, a southward filament from the central bulge, and a northward coastal current following the coastline, which generates small-scale eddies promoted by the bathymetry and morphology constraints, (Fig. 3a-c).

Under low river discharge (Fig. 3a), the offshore extension of the plume is about 18 km, the northward current is weak ($0.2\text{-}0.3\text{ m s}^{-1}$), and the plume front reaches the Cávado River mouth. In addition, a re-circulating bulge in the near-field region is detectable, slightly tilted northward with an approximate diameter of about 17 km. Under moderate river discharge (Fig. 3b), the Douro estuarine plume presents an offshore extension of about 22 km with a re-circulating bulge ($\sim 25\text{ km}$ of diameter) northward tilted and partially detached from the coast. A nearshore surface current towards the north is also observed ($> 0.2\text{ m s}^{-1}$). Salinity surface patterns present similar features under high river discharge (Fig. 3c), but with an increase of freshwater, mainly in the bulge region. The longitudinal extension of the plume is also similar ($\sim 23\text{ km}$), but the bulge is wider ($\sim 35\text{ km}$ in the major axis of the ellipse).

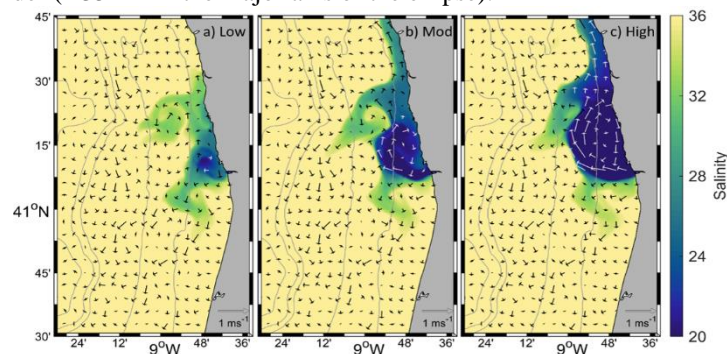


Fig. 3. Surface currents and salinity simulations 5 days after the peak river discharge (day 9) under low (a), moderate (b), and high (c) river discharges without wind.

3.3 Wind-driven Plume Dispersion

Surface salinity fields under the wind scenarios previously defined at moderate river discharge are depicted in Fig. 4. The time percentage from day 5 to 10 during which each grid cell has a salinity value < 30 is represented in the top-left corner of each panel. For the sake of simplicity, only the results under moderate river discharge and higher wind intensity are presented.

The maximum distance of offshore plume spreading is observed under upwelling-favorable (northerly) winds (Fig. 4a). In this case, the inclination observed between the main direction of the plume propagation and the river's mouth is influenced by an equilibrium between the river discharge and wind intensity. No re-circulating bulge is detectable, and the plume propagation exceeds the western boundary of the domain under moderate and high river discharges.

Surface salinity fields show plume confinement in the coastal region under southerly winds (Fig. 4b). The downwelling-favorable winds shrink the bulge near the river

mouth and the current speed towards north increases in comparison with simulations without wind (Fig. 3c). The offshore extension of the plume in front of the river mouth does not exceed ~ 10 km and ~ 6 km under moderate and high southerly winds, respectively. Combined with moderate-to-high river discharge, downwelling-favorable winds increase the possibility of the Douro plume to merge with estuarine sources located north of the estuary mouth, such as Minho estuarine plume [2].

The numerical scenario under easterly winds (Fig. 4c) shows a plume core detached from the coast and a weaker northward current (~ 0.3 m s $^{-1}$). The plume detachment is noticeable under strong winds, which push the plume offshore in opposition to the pressure gradient force, stopping the water re-circulation near the coast. The plume width near the mouth is larger under moderate (~ 15 km) than strong winds (~ 11 km), which can be explained by the reminiscent freshwater from the re-circulating bulge. However, the coastal plume is wider (~ 15 km) under strong than moderate wind intensities (~ 10 km).

Simulations under westerly winds (Fig. 4d) show the confinement of river plume landward, accumulating freshwater along the coast. Simulations under moderate and strong westerly winds show that the plume does not generate a buoyant coastal current northward.

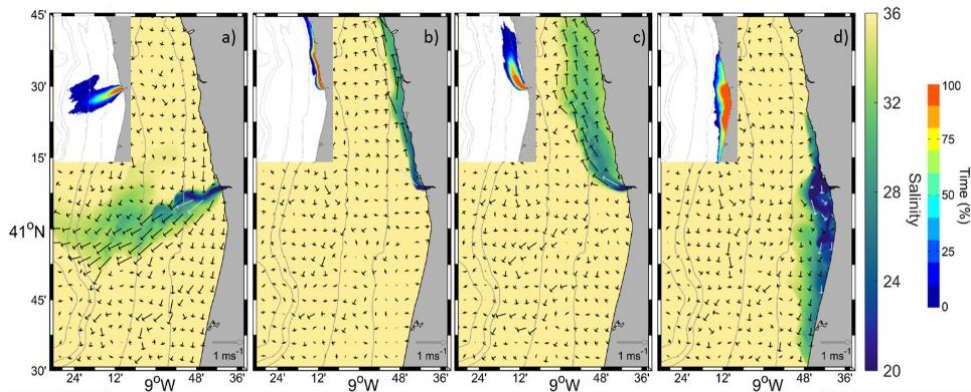


Fig. 4. Surface currents (ms $^{-1}$) and salinity 5 days after the peak discharge under moderate river discharge and strong northerly (a), southerly (b), easterly (c), and westerly wind (d). The top-left corner of each panel represents the time percentage during which each grid cell has a salinity value <30 .

4 Conclusions

The objective of this study was to characterize numerically the Douro estuarine plume dispersion regarding its dynamics, scale, and fate under different river discharges and wind conditions. Numerical simulations were carried out by means of MOHID previously validated in the area under study. The results obtained from this analysis suggest the following:

- Without wind forcing, the plume expands offshore, creating a re-circulating bulge. Low salinity waters are advected to the right due to the Coriolis force, and then the plume water flows northward.

- Easterly winds form a similar feature to the no-wind case. However, the low salinity band is detached from the coast, with an increase of the northward current.
- Westerly winds tend to accumulate freshwater to the coast and can decrease the momentum near the mouth. A southward coastal current is identified under strong winds and moderate and high river discharges.
- Northerly winds generate a large offshore extension of the plume. There is an increase of stratification, which turns more efficient the control of the plume fate by the wind.
- Southerly winds confine the plume to the coast, which propagates only as a coastal buoyant current northward.

Acknowledgments

RM benefits from doctoral and post-doctoral grants (SFRH/BD/79555/2011 and SFRH/BPD/115093/2016) given by the Portuguese Science Foundation (FCT). MCS and NV are funded by national funds (OE), through FCT, I.P., in the scope of the framework contract foreseen in the numbers 4, 5 and 6 of the article 23, of the Decree-Law 57/2016, of August 29, changed by Law 57/2017, of July 19. Thanks are due for the financial support to CESAM (UID/AMB/50017 - POCI-01-0145-FEDER-007638) to FCT/MCTES through national funds (PIDDAC), and the co-funding by the FEDER, within the PT2020 Partnership Agreement and Compete 2020.

References

- [1] R. D. Hetland, "Relating River Plume Structure to Vertical Mixing," *J. Phys. Oceanogr.*, vol. 35, no. 9, pp. 1667–1688, Sep. 2005.
- [2] R. Mendes, M. C. Sousa, M. DeCastro, M. Gómez-Gesteira, and J. M. Dias, "New insights into the Western Iberian Buoyant Plume: Interaction between the Douro and Minho River plumes under winter conditions," *Prog. Oceanogr.*, vol. 141, pp. 30–43, Feb. 2016.
- [3] M. C. Sousa, "Modelling the Minho River Plume Intrusion into the Rias Baixas," Universidade de Aveiro, 2013.
- [4] L. Carrère, F. Lyard, M. Cancet, A. Guillot, and L. Roblou, "FES2012: A new global tidal model taking advantage of nearly twenty years of altimetry," in *Proceedings of the 20 Years of Progress in Radar Altimetry Symposium*, 2012, pp. 1–20pp.
- [5] R. Flather, "A tidal model of the northwest European continental shelf," *Mem. Soc. R. Sci. Liege*, vol. 10, no. 6, pp. 141–164, 1976.
- [6] J. J. Becker *et al.*, "Global Bathymetry and Elevation Data at 30 Arc Seconds Resolution: SRTM30_PLUS," *Mar. Geod.*, vol. 32, no. 4, pp. 355–371, Nov. 2009.
- [7] M. M. Zweng *et al.*, "World Ocean Atlas 2013. Vol. 1: Salinity," in *NOAA Atlas NESDIS 74*, S. Levitus and A. Mishonov, Eds. 2013, p. 40pp.
- [8] E. A. Martinsen and H. Engedahl, "Implementation and testing of a lateral boundary scheme as an open boundary condition in a barotropic ocean model," *Coast. Eng.*, vol. 11, no. 5–6, pp. 603–627, Dec. 1987.
- [9] W. C. Skamarock *et al.*, "A description of the Advanced Research WRF Version 3," 2008.